

Early Metabolic Changes Due to Caloric Restriction in Rhesus Monkey Liver

Timothy W. Rhoads¹, Maggie S. Burhans¹, Paul D. Hutchins², Vincent B. Chen³, Sean J. McIlwain⁴,
Hamid R. Eghbalnia³, Irene M. Ong⁴, John L. Markley³, Joshua J. Coon², Rozalyn M. Anderson¹
Department of ¹Medicine, ²Chemistry, ³National Magnetic Resonance Facility, ⁴Biostatistics and Medical Informatics

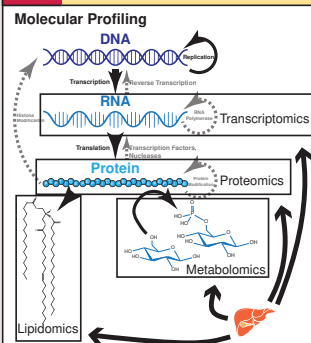
Introduction

Caloric Restriction (CR) without malnutrition delays aging and the incidence of age-related diseases in numerous model organisms, from yeast to primates. Although components of the mechanism in many organisms are beginning to emerge, a comprehensive understanding of how CR impacts the aging process in higher organisms, especially humans, is currently lacking. The Wisconsin National Primate Research Center (WNPRC) began a long-term study of CR in rhesus macaque monkeys in 1989 to address this deficit. Results from this study, previously published, describe how CR lowers all-cause mortality and increases longevity. Importantly, tissue biopsies were collected from these animals at various time points throughout the study, providing a means to investigate the molecular mechanisms underlying the beneficial effects of CR on aging.

Here, we examine the early trajectory of CR by analyzing liver biopsies collected from the monkeys at study enrollment and after two years of the diet regimen. Using a systems biology approach, which attempts to comprehensively describe the state of the whole system rather than the individual pieces, we assessed molecular profiles comprising five different molecule types: messenger RNA via high-throughput RNA sequencing, metabolomics via NMR, proteomics and post-translational modification with acetylation via mass spectrometry, and large-scale lipid composition analysis via mass spectrometry. These data represent quantification of over 20,000 biological molecules from the livers of five control and 5 CR monkeys. We show that CR induces a distinct metabolic signature, affecting branched-chain amino acid metabolism, lipid metabolism, and RNA processing, among others, while strongly influencing the mitochondria, the powerhouses of the cell. We also describe the concordance/discordance between subsets of transcripts and proteins, lending insight into components of the mechanism regulated pre- and post-translationally.

These data reveal a metabolic program that is induced by CR very early on in the diet routine, indicating that downstream aging processes may also be set in motion long before phenotypic effects are clinically observed. As such, this study has yielded a multitude of targets and hypotheses to investigate for anti-aging interventions that will be pursued for follow-up.

Methods



Liver biopsies were collected from control and restricted monkeys at study enrollment and after two years of the diet regime.

Figure 1. Molecular Profiling. We used high throughput molecular profiling technologies to profile 5 different classes of molecules: messenger RNA transcripts with next generation sequencing, proteins and acetyl protein post-translational modifications with mass spectrometry, lipids with mass spectrometry, and metabolites with nuclear magnetic resonance spectroscopy. This results in quantitative profiles of over 20,000 biological molecules.

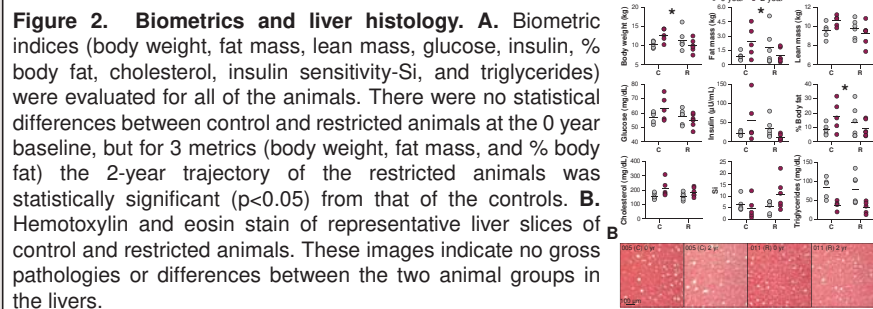
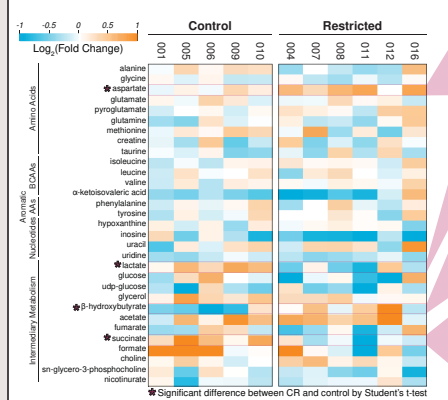


Figure 2. Biometrics and liver histology. **A.** Biometric indices (body weight, fat mass, lean mass, glucose, insulin, % body fat, cholesterol, insulin sensitivity-Si, and triglycerides) were evaluated for all of the animals. There were no statistical differences between control and restricted animals at the 0 year baseline, but for 3 metrics (body weight, fat mass, and % body fat) the 2-year trajectory of the restricted animals was statistically significant ($p < 0.05$) from that of the controls. **B.** Hematoxylin and eosin stain of representative liver slices of control and restricted animals. These images indicate no gross pathologies or differences between the two animal groups in the livers.

Results

Metabolomics



Proteomics

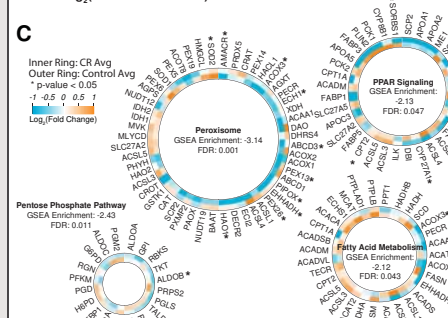
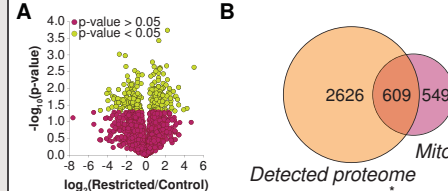
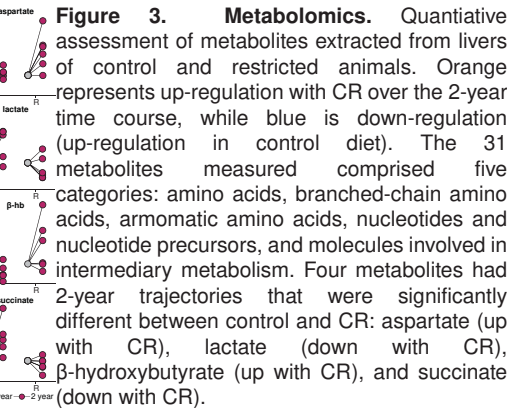


Figure 5. Proteomics. **A.** Volcano plot of every protein p-value vs. the \log_2 fold change. Statistically significant proteins are in yellow, 254 proteins out of a total of 3,243. **B.** Venn diagram describing the quantification of 609 (~52%) mitochondrial proteins, according to MitoCarta. **C.** Circular heat maps of cellular pathways found to be significantly over-represented (relative to the whole proteome) in the dataset. The inner ring is the average of the two-year trajectory of four restricted animals, while the outer ring is the same for control animals.



Acetyl-proteomics

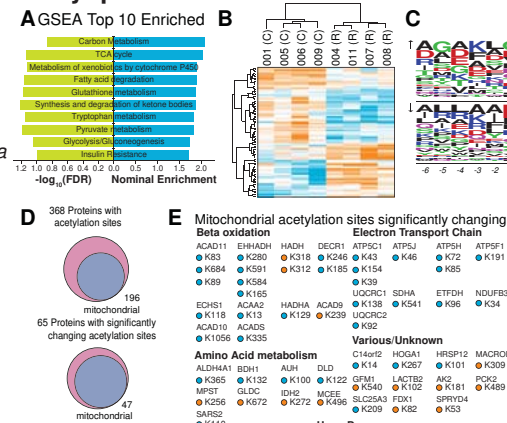


Figure 6. Acetyl-proteomics. **A.** Bar graph showing the top 10 pathways over-represented in the acetyl-proteome dataset, ranked by p-value and enrichment (the fold increase of the number of genes from the pathway present in the dataset, divided by the number of genes expected, given the size of the whole dataset). **B.** Heatmap showing the two-year trajectories of the significantly changing acetyl-proteome forms ($p < 0.05$). In general, acetylation is down in restricted animals. **C.** Schematic representing the amino acid sequence surrounding acetyl sites upregulated with CR (top) and down-regulated (bottom) with CR. There appears to be a slight preference for basic amino acids (K, R) in those down in CR. **D.** Venn diagrams describing the proportion of all (top), and significant (bottom) acetyl sites that are mitochondrial. An overwhelming number (>50%) are mitochondrial. **E.** Table of all mitochondrial acetyl sites significantly changing. Blue are sites down-regulated with CR orange are up-regulated with CR.

Lipidomics

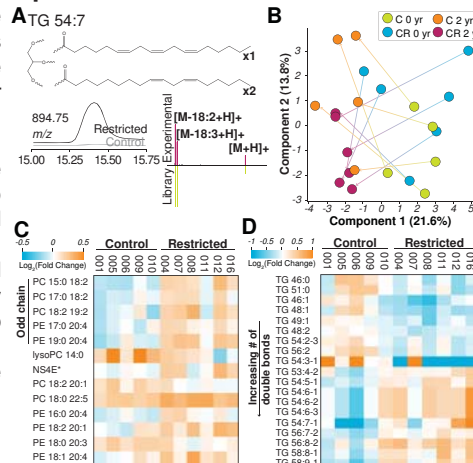


Figure 4. Lipidomics. **A.** Example of mass spectrometry analysis of lipids. **B.** Principal Component Analysis (PCA) of all lipids. This describes the variance between all of the animals in terms of specific components; the spread of the animals and the direction they move over the 2-year diet period can be observed in this analysis. **C** and **D.** Heat maps of lipids with significantly different 2-year trajectories between control and restricted. Dividing the lipids into phospholipids and triglycerides reveals upregulation of odd chain phospholipids and highly unsaturated triglycerides in restricted animals.

Transcriptomics

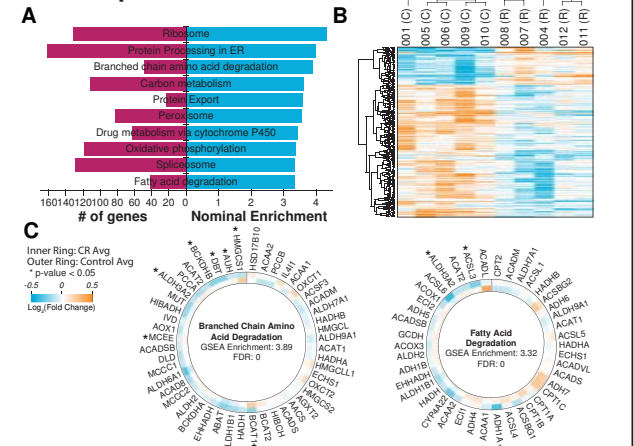


Figure 7. Transcriptomics. **A.** Bar graph showing the top 10 over-represented cellular pathways represented in the messenger RNA dataset, ranked by the number of genes found from the pathway and the pathway enrichment. **B.** Heatmap showing the significantly changing mRNA transcripts. The bulk of the ~400 transcripts are down-regulated over the two-year period in restricted animals. **C.** Circular heat maps of cellular pathways found to be significantly over-represented (relative to the whole transcriptome) in the dataset. The inner ring is the average of the two-year trajectory of four restricted animals, while the outer ring is the same for control animals.

Conclusions

These data, the profiling of greater than 20,000 biological molecules, demonstrate that CR initiates the induction of a substantial metabolic reprogramming observable across many different classes of molecules; this reprogramming dramatically effects the mitochondria, lipid metabolism, mRNA splicing, and energy metabolism, and is clearly present early in the diet regime, presaging the longevity benefits that CR can provide.

Acknowledgements and References

We are grateful to Priya Balsubramanian and Thomas Pugh for assistance with histology. This work was funded by NIH National Institute of Aging.

Colman, R.J., Anderson, R.M., Johnson, S.C., et al. (2009). Caloric restriction delays disease onset and mortality in rhesus monkeys. *Science* 325, 201-204.
Calvo, S.E., Clauser, K.R., and Mootha, V.K. (2016). MitoCarta2.0: an updated inventory of mammalian mitochondrial proteins. *Nucleic Acids Res* 44, D1251-1257.